Performance Analysis of Polarization-Insensitive Phase Diversity Optical FSK Receivers

HEN-WAI TSAO, STUDENT MEMBER, IEEE, JINGSHOWN WU, MEMBER, IEEE, SHIEN-CHI YANG, AND YANG-HAN LEE

Abstract—**A polarization-insensitive phase-diversity optical frequency-shift-keying (FSK) receiver is proposed and its performance is also evaluated. The basic model and signal processing formulation are developed to describe the functions and features of this receiver. Two different approaches (one of which is an upper bound) are used to treat the mixed noise terms, and Gaussian approximation is employed to estimate the receiver performance in terms of the laser linewidth, the modulation index, and the filter bandwidth. The virtually polarization-insensitive property is also verified. As an example, numerical results are presented for a 150-Mbit/s receiver, which show that the difference between the upper bound and the other approximation is about 2 to 3 dB. It is also shown that the receiver with small modulation index is less tolerant of the linewidth such that an error floor may appear. When the modulation index is large, the receiver can tolerate linewidths comparable with the bit rate.**

I. Introduction

COHERENT optical transmission has received much attention because of higher sensitivity and many other potential advantages over intensity modulation/direct detection (IM/DD) systems [1]. Among many possible coherent transmission schemes, frequency shift keying (FSK) is of great importance for 1) it imposes less stringent requirement on the laser linewidths than phase shift keying (PSK) and differential phase shift keying (DPSK) [2] and commercially available DFB semiconductor lasers can be used, 2) the modulated lightwave has a constant envelope to allow the fiber (and possibly, optical amplifiers) to handle much larger power [1], and 3) a large frequency deviation can be used to combat the degradation due to large linewidth. Most of the FSK optical receivers investigated [2]–[5] are of the heterodyne structure. However, the zero-IF phase-diversity scheme [6], [7] has the advantage of directly processing the relatively low frequency baseband signals. This may alleviate many hardware problems when high bit rate and large frequency deviation are employed.

In a coherent optical receiver it is also important that the received and locally generated demodulating optical field must have the same polarization. To achieve this purpose we may [1] 1) use a polarization maintaining fiber, 2) employ some adaptive polarization correction schemes, or 3) adopt a more complicated "polarization-insensitive" receiver structure [8], [9] whose performance is relatively independent of the extent to which the polarizations of the received and local fields are matched.

In this paper we analyze the performance of a polarization-insensitive phase-diversity optical FSK receiver. In Section II the receiver structure is described. Expressions for the output of frequency discriminators have been obtained. In Section III, we first evaluate the noise power by using two slightly different approximations for the "mixed" noise terms. Then we calculate the bit error rate (BER) based on each of the two approximations and the assumption that the total error statistics are approximately Gaussian, which is partially checked by simulation as shown in the Appendix. The BER expressions for the "single branch" (i.e., no polarization diversity) receiver are also obtained as a special case. In Section IV numerical results are obtained for a medium-speed data link with various frequency deviation and total linewidth values. These results demonstrate the satisfactory performance of this receiver despite its more complicated structure. In particular, significant linewidths can be tolerated provided the frequency deviation is large and the local oscillator power is strong enough to suppress the thermal noise.

II. Basic System Configuration and Signal Processing

The block diagram of the polarization-insensitive phase diversity optical FSK receiver is shown in Fig. 1. The received optical signal $E_s(t)$ is split into one horizontally polarized and another vertically polarized beam by a suitable device (such as a Wollaston prism, $WP_{(a)}$). The local oscillator output $E_L(t)$ is also split by a similar device ($WP_{(b)}$) into two beams that have the same polarization as the two outputs of $WP_{(a)}$, respectively. Two identical optical hybrids are then employed to combine the vertically and horizontally polarized received and local oscillator (LO) signals so that at the outputs of the first ("vertical") hybrid are

$$E_{1i} = \sqrt{P_s\beta_1^2}\cos\left(\omega_c t + \phi_m(t) + \phi_T(t) + \alpha_1\right) + \sqrt{P_L/2}\cos\left(\omega_c t + \phi_L(t) + \delta_1\right) \quad (1a)$$

Manuscript received March 3, 1989; revised September 12, 1989. This work was supported by the National Science Council of the Republic of China under Grant NSC 78-0417-E002-07.

The authors are with the Department of Electrical Engineering, National Taiwan University, Taipei, Taiwan 10764, Republic of China.

IEEE Log Number 8932779.

0733-8724/90/0300-0385$01.00 © 1990 IEEE

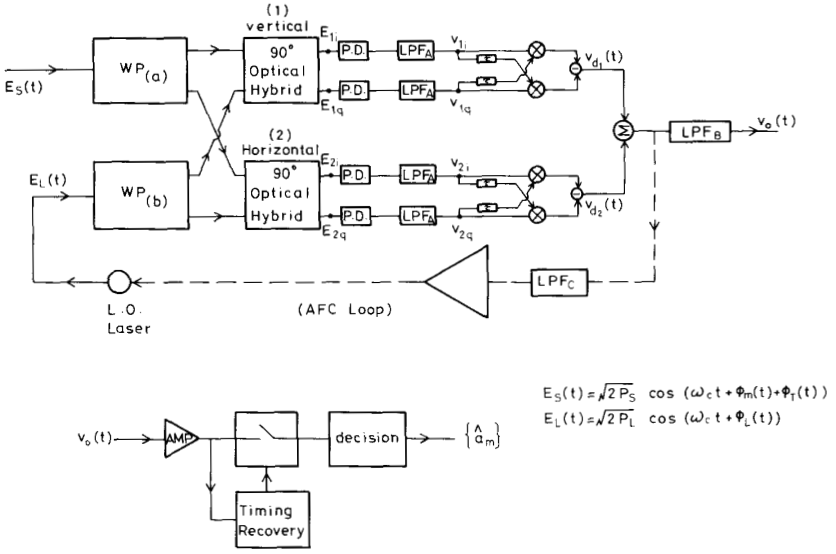

Fig. 1. Block diagram of the polarization-insensitive phase-diversity optical FSK receiver.

and

$$E_{1q} = \sqrt{P_s\beta_1^2}\cos\left(\omega_c t + \phi_m(t) + \phi_T(t) + \alpha_1\right) + \sqrt{P_L/2}\sin\left(\omega_c t + \phi_L(t) + \delta_1\right) \quad (1b)$$

while the outputs of the second ("horizontal") hybrid are

$$E_{2i} = \sqrt{P_s\beta_2^2}\cos\left(\omega_c t + \phi_m(t) + \phi_T(t) + \alpha_2\right) + \sqrt{P_L/2}\cos\left(\omega_c t + \phi_L(t) + \delta_2\right) \quad (2a)$$

and

$$E_{2q} = \sqrt{P_s\beta_2^2}\cos\left(\omega_c t + \phi_m(t) + \phi_T(t) + \alpha_2\right) + \sqrt{P_L/2}\sin\left(\omega_c t + \phi_L(t) + \delta_2\right) \quad (2b)$$

where P_s is the received signal power, P_L is the LO power, β_1^2 is the fraction of P_s in the horizontal direction, β_2^2 is the fraction of P_s in the vertical direction, $\phi_m(t)$ is the phase modulation due to message signal, $\phi_T(t)$ and $\phi_L(t)$ are the phase noises of transmitting and LO lasers, ω_c is the carrier and LO frequency (assumed identical), and α_1, α_2, δ_1, and δ_2 are the phase angles representing different optical lengths.

It has also been assumed that the LO output is aligned in such a way as to produce equal power in horizontal and vertical directions.

The four outputs from the two horizontal and vertical optical hybrids are then converted to electric signals by four identical optic-electric (O-E) converters consisting of p-i-n diodes (with responsivity R A/W) followed by low noise preamplifiers and equalizers (with overall transimpedance value 1 Ω). Identical low-pass filters, LPF_A, are used in each "arm" to remove the high frequency noise while leaving the signal components virtually unchanged. At the low-pass filter outputs we have

$$v_{1i} = C_1\cos\left(\phi_m(t) + \phi_T(t) - \phi_L(t) + \alpha_1 - \delta_1\right) + n_{1i}(t) \quad (3a)$$

$$v_{1q} = -C_1\sin\left(\phi_m(t) + \phi_T(t) - \phi_L(t) + \alpha_1 - \delta_1\right) + n_{1q}(t) \quad (3b)$$

and

$$v_{2i} = C_2\cos\left(\phi_m(t) + \phi_T(t) - \phi_L(t) + \alpha_2 - \delta_2\right) + n_{2i}(t) \quad (4a)$$

$$v_{2q} = -C_2\sin\left(\phi_m(t) + \phi_T(t) - \phi_L(t) + \alpha_2 - \delta_2\right) + n_{2q}(t) \quad (4b)$$

where all dc terms have been omitted since they will have no contribution to the discriminator output, and

$$C_k \triangleq R\sqrt{P_s P_L\beta_k^2/2}, \qquad k = 1, 2. \quad (5)$$

$n_{1i}(t)$, $n_{1q}(t)$, $n_{2i}(t)$, and $n_{2q}(t)$ are shot noises generated in the photodetection process.

It is assumed that P_L is much larger than P_s and all thermal noises in electronic circuits are negligible. Thus $n_{1i}(t)$, $n_{1q}(t)$, $n_{2i}(t)$, and $n_{2q}(t)$ are all zero-mean independent Gaussian processes with double-sided power spectral density (PSD)

$$N_0 = \frac{qRP_L}{4} \quad (6)$$

up to the cutoff frequency of the low-pass filter, LPF_A.

Two identical delay-and-multiplying discriminators [7] are used in the horizontal and vertical "branches" to pro-

duce two separate "detected" outputs $v_{d1}(t)$ and $v_{d2}(t)$ as follows:

$$v_{d1}(t) = v_{1i}(t)v_{1q}(t-\tau) - v_{1i}(t-\tau)v_{1q}(t) \quad (7a)$$

$$v_{d2}(t) = v_{2i}(t)v_{2q}(t-\tau) - v_{2i}(t-\tau)v_{2q}(t). \quad (7b)$$

Substituting (3a), (3b), (4a), and (4b) into (7a) and (7b) and using the fact that, for practical implementation, τ is much smaller than the bit duration T [7], we may expand the resulting expression in a power series of τ and retain only the first-order terms. The final results are [10]

$$\begin{aligned} v_{dk}(t) = {} & C_k^2\left(2\pi f_d m(t)\tau + 2\pi f_N(t)\tau\right) \\ & + C_k\tau\Big\{n_{ki}(t)\left(\phi_m'(t) + \phi_N'(t)\right) \\ & \cdot \cos\left(\phi_m(t) + \phi_N(t) + \alpha_k - \delta_k\right) \\ & - n_{kq}(t)\left(\phi_m'(t) + \phi_N'(t)\right)\sin\left(\phi_m(t)\right. \\ & \left. + \phi_N(t) + \alpha_k - \delta_k\right) - n_{ki}'(t)\sin\left(\phi_m(t)\right. \\ & \left. + \phi_N(t) + \alpha_k - \delta_k\right) - n_{kq}'(t)\cos\left(\phi_m(t)\right. \\ & \left. + \phi_N(t) + \alpha_k - \delta_k\right)\Big\} \\ & + \tau\left\{n_{ki}'(t)\, n_{kq}(t) - n_{ki}(t)n_{kq}'(t)\right\}, \\ & k = 1, 2. \end{aligned} \quad (8)$$

In deriving (8), we have assumed that

$$\phi_m(t) = 2\pi f_d \int_0^t m(\alpha)d\alpha, \qquad \left|m(t)\right|_{\max} = 1 \quad (9)$$

where $m(t)$ is the baseband message signal and we have also defined the "combined" phase noise $\phi_N(t)$ and frequency noise $f_N(t)$ to be

$$\begin{aligned} \phi_N(t) &\triangleq \phi_T(t) - \phi_L(t) \\ &= 2\pi \int_0^t f_N(\alpha)d\alpha. \end{aligned} \quad (10)$$

$f_N(t)$ has been shown to be well approximated by a white Gaussian zero-mean process with double-sided PSD [11]

$$S_{fN}(f) = \frac{\Delta\nu}{2\pi} \quad (11)$$

where $\Delta\nu = \Delta\nu_T + \Delta\nu_L$ is the "total" linewidth.

Since the modulating signal $m(t)$ is usually band limited to a frequency f_m, it is advantageous to add a low-pass filter LPF_B to eliminate the "out-of-band" noise in the combined detected signal $v_{d1}(t) + v_{d2}(t)$. The final decision of the transmitted data is therefore based on

$$v_0(t) = \text{LPF}_B\left\{v_{d1}(t) + v_{d2}(t)\right\}. \quad (12)$$

III. Performance Analysis

A. Signal and Noise Power Estimation

To analyze the system performance, the following observations and assumptions are made at the beginning.

1) The message signal $m(t)$ is of the form

$$m(t) = \sum_{k=-\infty}^{\infty} a_k P(t - kT) \quad (13)$$

where $a_k = \pm 1$ and $\{a_k\}_k^{\infty} = -\infty$ is the transmitted data sequence with $\Pr\{a_k = \pm 1\} = 1/2$ and $E\{a_k a_s\} = 0$ for $k \neq s$. $p(t)$ is the transmitted pulse waveform satisfying the Nyquist criterion [12] $p(0) = 1$ and $p(mT) = 0$ for nonzero integer m. The raised cosine pulse is a good example.

2) $v_{dk}(t)$, $k = 1, 2$, may be separated into signal and various noise components as

$$\begin{aligned} v_{dk}(t) &= s_{dk}(t) + n_{dk}(t) \\ &= s_{dk}(t) + \left(n_{df,k}(t) + n_{d\text{mix},k}(t) + n_{d\text{shot},k}(t)\right) \end{aligned} \quad (14)$$

where

$$\begin{aligned} s_{dk}(t) &= C_k^2\tau\ (2\pi f_d)m(t) \\ n_{df,k}(t) &= C_k^2\tau\ 2\pi f_N(t) \\ n_{d\text{mix},k}(t) &= C_k\tau\ \Big\{n_{ki}(t)\left(\phi_m'(t) + \phi_N'(t)\right)\cos\left(\phi_m(t)\right. \\ &\quad \left. + \phi_N(t) + \alpha_k - \delta_k\right) \\ &\quad -n_{kq}(t)\left(\phi_m'(t) + \phi_N'(t)\right)\sin\left(\phi_m(t)\right. \\ &\quad \left. + \phi_N(t) + \alpha_k - \delta_k\right) \\ &\quad -n_{ki}'(t)\sin\left(\phi_m(t) + \phi_N(t) + \alpha_k - \delta_k\right) \\ &\quad - n_{kq}'(t)\cos\left(\phi_m(t)\right. \\ &\quad \left. +\phi_N(t) + \alpha_k - \delta_k\right)\Big\} \\ n_{d\text{shot},k}(t) &= \tau\left\{n_{ki}'(t)n_{kq}(t) - n_{ki}(t)n_{kq}'(t)\right\}. \end{aligned} \quad (18)$$

3) The bandwidth of the LPF_A is chosen according to Carson's rule [13], $f_A \triangleq (\beta + 1)f_m$, where f_m is the bandwidth of $m(t)$, and $\beta = f_d/f_m$ is the modulation index (or deviation ratio). The shot noises $n_{ki}(t)$, $n_{kq}(t)$, $k = 1, 2$, are, therefore, also band limited to f_A.

4) The noise processes $n_{ki}(t)$, $n_{kq}(t)$, $k = 1, 2$, and $f_N(t)$ are all mutually independent and also independent of the message signal $m(t)$. We also have

$$E\left\{n_{ki}'(t)n_{ki}(t)\right\} = E\left\{n_{kq}(t)n_{kq}'(t)\right\} = 0, \qquad k = 1, 2. \quad (19)$$

5) The timing recovery circuit works perfectly in the presence of noise so that the sampling instants occur at $t = mT$, where m is an integer, exactly.

Under the above assumptions and using Gaussian approximation for the detector output signal, we may now determine the statistics of the sampled value of $v_0(t)$, $v_0(mT)$.

To find the mean of $v_0(mT)$, we note that $v_0(t) = \text{LPF}_B\{v_{d1}(t) + v_{d2}(t)\}$ and since $m(t)$ is band limited to the frequency $f_m (f_m \leq 1/T$ if $p(t)$ is a raised cosine

pulse) which is taken to be the cutoff frequency of the ideal low-pass filter LPF_B, the filtering has no effect on the signal component in $v_{d1}(t)$ and $v_{d2}(t)$. Hence

$$s_0(t) = s_{d1}(t) + s_{d2}(t) \tag{20}$$

and

$$\begin{aligned} E\{v_0(mT)\} &= s_0(mT) = s_{d1}(mT) + s_{d2}(mT) \\ &= (C_1^2 + C_2^2)\,\tau(2\pi f_d)a_m \\ &= \pm C^2\tau\,(2\pi f_d) \end{aligned} \tag{21}$$

where we have used the fact that all noise terms in $v_{dk}(t)$, $k = 1, 2$, have zero mean and $p(t)$ satisfies the Nyquist criterion. We also define

$$C \triangleq \sqrt{C_1^2 + C_2^2} = R\sqrt{\frac{P_s P_L}{2}} \tag{22}$$

assuming that $\beta_1^2 + \beta_2^2 = 1$.

To find the variance of $v_0(mT)$, we first note that

$$\begin{aligned} \mathrm{var}\{v_0(mT)\} &= \mathrm{var}\left\{\sum_{k=1}^{2}\left(n_{0f,k}(mT) + n_{0\mathrm{mix},k}(mT) + n_{0\mathrm{shot},k}(mT)\right)\right\} \\ &= E\left\{\left(n_{0f,1}(mT) + n_{0f,2}(mT)\right)^2\right\} \\ &\quad + \sum_{k=1}^{2} E\{n_{0\mathrm{mix},k}^2(mT)\} \\ &\quad + \sum_{k=1}^{2} E\{n_{0\mathrm{shot},k}^2(mT)\} \end{aligned} \tag{23}$$

where it is easy to verify that all the cross terms vanish. Equation (23) shows that we can consider the contribution of each noise term separately.

1) The Frequency Noise $n_{0f}(t) = n_{0f,1}(t) + n_{0f,2}(t)$: Since

$$\begin{aligned} n_{0f,k}(t) &= \mathrm{LPF}_B\{n_{df,k}(t)\}, \qquad k = 1, 2 \\ &= C_k^2\tau\; 2\pi\; \mathrm{LPF}_B\{f_N(t)\} \end{aligned} \tag{24}$$

we have

$$n_{0f}(t) = C^2\tau\; 2\pi\; \mathrm{LPF}_B\{f_N(t)\} \tag{25}$$

and

$$\begin{aligned} E\{n_{0f}^2(mT)\} &= C^4\tau^2(2\pi)^2\int_{-f_m}^{f_m}\frac{\Delta\nu}{2\pi}\,df \\ &= C^4\tau^2(4\pi^2)\frac{\Delta\nu}{\pi}f_m. \end{aligned} \tag{26}$$

2) The Mixed Noise, $n_{0mix,k}(t)$, $k = 1, 2$: $n_{0\mathrm{mix},k}(t)$, $k = 1, 2$, are the low-pass filtered versions of $n_{0\mathrm{mix},k}(t)$. Since $n_{d\mathrm{mix},k}(t)$, $k = 1, 2$, are non-Gaussian nonstationary processes, exact evaluation of their power at the output of LPF_B is very difficult. We thus try to obtain two slightly different approximations based on some simplifying assumptions.

Approximation I: The simplifying assumptions are as follows:

a) The effect of LPF_B is simply to limit the wide-band noise terms ($n_{ki}(t)$, $n_{kq}(t)$, $\phi_N'(t) = 2\pi f_N(t)$, $n_{ki}'(t)$, $n_{kq}'(t)$, etc.) in $n_{d\mathrm{mix},k}(t)$ to the bandwidth f_m (in the order of $1/T$). The mathematical forms of $n_{0\mathrm{mix},k}(t)$, $k = 1, 2$, are approximately unchanged.

b) The message signal $m(t) = \sum_{k=-\infty}^{\infty} a_k p(t - kT)$ is approximated as a stationary process with zero mean ($E\{a_k\} = 0$) and PSD $|P(f)|^2 T$ [14], where $P(f)$ is the Fourier transform of $p(t)$. $m(t)$ is, of course, independent of other noise terms in $n_{d\mathrm{mix},k}(t)$.

Under the assumptions stated in a) and b), we can derive

$$\begin{aligned} &E\{n_{0\mathrm{mix}}^2(t)\} \\ &\quad = E\{n_{0\mathrm{mix},1}^2(t)\} + E\{n_{0\mathrm{mix},2}^2(t)\} \\ &\quad = C^2\tau^2 4\pi^2\left\{2N_0 f_m\left(f_d^2\overline{m^2(t)} + \frac{\Delta\nu\cdot f_m}{\pi}\right) + \frac{2}{3}N_0 f_m^3\right\} \\ &\quad = 8C^2\tau^2\pi^2 N_0 f_m\left\{\left(f_d^2\overline{m^2(t)} + \frac{\Delta\nu\cdot f_m}{\pi}\right) + \frac{1}{3}f_m^2\right\}. \end{aligned} \tag{27}$$

Approximation II: In this approximation, we define

$$\begin{aligned} \bar{n}_{d\mathrm{mix},k} = C_k\tau\{&n_{ki}(t)(\phi_m'(t) + \phi_N'(t)) \\ &- n_{kq}(t)(\phi_m'(t) + \phi_N'(t)) \\ &- n_{ki}'(t) - n_{kq}'(t)\}, \qquad k = 1, 2. \end{aligned} \tag{28}$$

$\bar{n}_{d\mathrm{mix},k}(t)$ may be taken as an "upper bound" for $n_{d\mathrm{mix},k}(t)$, $k = 1, 2$. Since it is a stationary process, its power spectral density may be found, and at the output of LPF_B, we have an upper bound for $E\{n_{0mix}^2(t)\}$ at any t as

$$\begin{aligned} &E\{\bar{n}_{0\mathrm{mix}}^2(t)\} \\ &\quad = E\{\bar{n}_{0\mathrm{mix},1}^2(t)\} + E\{\bar{n}_{0\mathrm{mix},2}^2(t)\} \\ &\quad = 2C^2\tau^2 4\pi^2\left\{2N_0 f_m\left[f_d^2\overline{m^2(t)} + \frac{\Delta\nu f_m}{4\pi}(4\beta + 3)\right] + \frac{2}{3}N_0 f_m^3\right\} \\ &\quad = 16C^2\tau^2\pi^2 N_0 f_m\left\{f_d^2\overline{m^2(t)} + \frac{\Delta\nu f_m}{4\pi}(4\beta + 3) + \frac{1}{3}f_m^2\right\}. \end{aligned} \tag{29}$$

In deriving (29), we have assumed that $\beta > 1$.

3) The Shot Noise $n_{0shot}(t) = n_{0shot,1}(t) + n_{0shot,2}(t)$: $n_{0\mathrm{shot},k}(t)$, $k = 1, 2$, are the low-pass filtered versions of $n_{d\mathrm{shot},k}(t)$. We need only consider $k = 1$, for the two terms are independent and identically distributed.

We define

$$n'_{1i}(t)n_{1q}(t) \triangleq n_{1A}(t) \tag{30a}$$

$$n'_{1i}(t)n_{1q}(t) \triangleq n_{1B}(t) \tag{30b}$$

Then

$$n_{d\text{shot},1}(t) = \tau(n_{1A}(t) - n_{1B}(t)) \tag{31}$$

$$\begin{aligned} R_{d\text{shot},1}(\tau) &= E\{n_{d\text{shot},1}(t)n_{d\text{shot},1}(t+\tau)\} \\ &= \tau^2\{R_{n_{1A}}(\tau) + R_{n_{1B}}(\tau) - R_{n_{1A}n_{1B}}(\tau) \\ &\quad - R_{n_{1A}n_{1B}}(-\tau)\}. \end{aligned} \tag{32}$$

But

$$\begin{aligned} R_{n_{1A}}(\tau) &= E\{n'_{1i}(t)n'_{1i}(t+\tau)\}E\{n_{1q}(t)n_{1q}(t+\tau)\} \\ &= \left[-\frac{d^2}{d\tau^2}R_{n_{1i}}(\tau)\right][R_{n_{1q}}(\tau)] \end{aligned} \tag{33}$$

so

$$S_{n_{1A}}(f) = (4\pi^2 f^2 S_{n_{1i}}(f)) * (S_{n_{1q}}(f)). \tag{34}$$

Similarly, we find

$$S_{n_{1B}}(f) = (4\pi^2 f^2 S_{n_{1q}}(f)) * (S_{n_{1i}}(f)) \tag{35}$$

and

$$\begin{aligned} S_{n_{1A}n_{1B}}(f) = S_{n_{1B}n_{1A}}(f) &= 4\pi^2(fS_{n_{1i}}(f)) \\ &\quad * (fS_{n_{1q}}(f)). \end{aligned} \tag{36}$$

Thus

$$\begin{aligned} S_{n_d\text{shot},1}(f) &= \tau^2 4\pi^2[(f^2 S_{n_{1i}}(f)) * (S_{n_{1q}}(f)) \\ &\quad + (f^2 S_{n_{1q}}(f)) * (S_{n_{1i}}(f)) \\ &\quad - 2(fS_{n_{1i}}(f)) * (fS_{n_{1q}}(f))] \end{aligned} \tag{37}$$

and therefore

$$\begin{aligned} &E\{n^2_{0\text{shot},1}(t)\} \\ &= \int_{-fm}^{fm} S_{n_d\text{shot},1}(f)\,df \\ &= \frac{4\pi^2}{3}N_0^2 f_m^4\left[16\beta^3 + 36\beta^2 + 28\beta + \frac{15}{2}\right]\tau^2 \\ &= E\{n^2_{0\text{shot},2}(t)\}. \end{aligned} \tag{38}$$

B. Bit Error Rate Calculation Based on Gaussian Approximation

1) BER According to Approximation I of "Mixed" Noise: Using (21), (26), (27), and (38), we have

$$P_e \approx Q\left[\frac{\beta}{\left\{\frac{\Delta\nu}{\pi f_m} + \left(\frac{qf_m}{RP_s}\right)\left[\beta^2\overline{m^2(t)} + \frac{\Delta\nu}{\pi f_m} + \frac{1}{3}\right] + \frac{1}{6}\left(\frac{qf_m}{RP_s}\right)^2\left(16\beta^3 + 36\beta^2 + 28\beta + \frac{15}{2}\right)\right\}^{1/2}}\right]. \tag{39}$$

2) BER According to Approximation II (Upper Bound) of "Mixed" Noise: Using (21), (26), (29), and (38). We have

$$P_e \approx Q\left[\frac{\beta}{\left\{\frac{\Delta\nu}{\pi f_m} + 2\left(\frac{qf_m}{RP_s}\right)\left[\beta^2\overline{m^2(t)} + \frac{\Delta\nu}{4\pi f_m}(4\beta + 3) + \frac{1}{3}\right] + \frac{1}{6}\left(\frac{qf_m}{RP_s}\right)^2\left(16\beta^3 + 36\beta^2 + 28\beta + \frac{15}{2}\right)\right\}^{1/2}}\right]. \tag{40}$$

3) BER for the Single Branch (i.e., no polarization diversity) Receiver: If polarization alignment at the receiver is achieved by other means, polarization diversity is unnecessary. Our receiver then reduces to the conventional phase-diversity receiver [7]. Its analysis is quite similar to that carried out above. The final BER expressions based on two approximations of $n_{d\text{mix}}(t)$ have the same form as (39) and (40) except that the coefficient of the last term in the denominator of the argument of Q-function is $1/12$ rather than $1/6$.

IV. Numerical Example

The following parameters are assumed for a typical medium-speed digital data link:

data rate = 150 Mbits/s;
photodetector responsivity (R) = 0.84 A/W;
frequency deviation (f_d) = 275 MHz (case A), 550 MHz (case B);
total linewidth ($\Delta\nu$) = 0, 1, 10, 30, 60, 100 MHz;
local oscillator power (P_L): large enough so that the thermal noise can be neglected;
pulse shaping: raised cosine, $\overline{m^2(t)} \approx 1$.

The BER's were computed using Gaussian approximation in case A (f_d = 275 MHz) and case B (f_d = 550 MHz) as a function of received power P_s for various total linewidth values listed above. Two sets of curves have been obtained in each case, based on the two different approximations employed in evaluating the power of the "mixed" noise terms.

Several facts are highlighted in the numerical results.

1) The two different approximations for the "mixed" noise terms in each case (Figs. 2 and 3 for case A; Figs. 4 and 5 for case B) result in a difference in P_s of 2–3 dB. Since Approximation I tends to underestimate the noise power, while Approximation II is an upper bound, the exact average BER should lie between the two sets of curves.

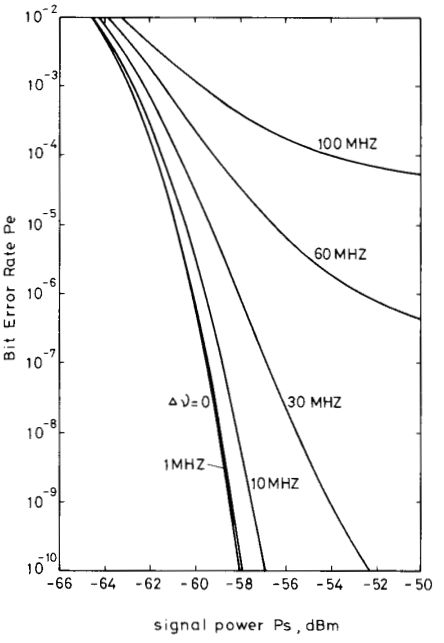

Fig. 2. BER curves for 150-Mbit/s data rate, 275-MHz frequency deviation, and Approximation I of the mixed noise terms.

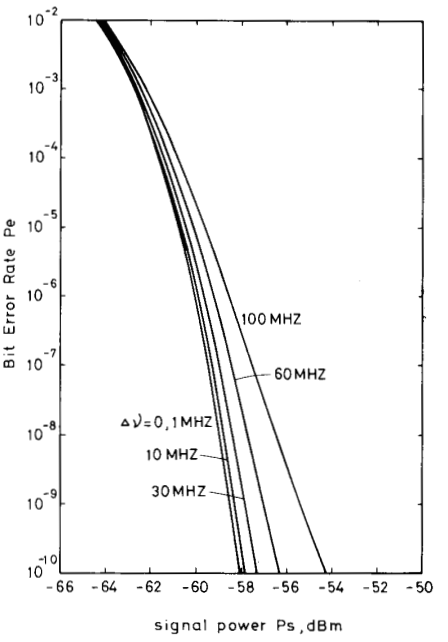

Fig. 4. BER curves for 150-Mbit/s data rate, 550-MHz frequency deviation and Approximation I of the mixed noise terms.

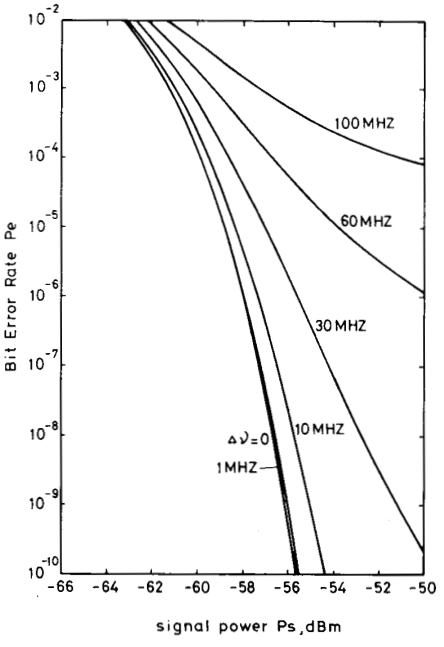

Fig. 3. BER curves for 150-Mbit/s data rate, 275-MHz frequency deviation, and Approximation II of the mixed noise terms.

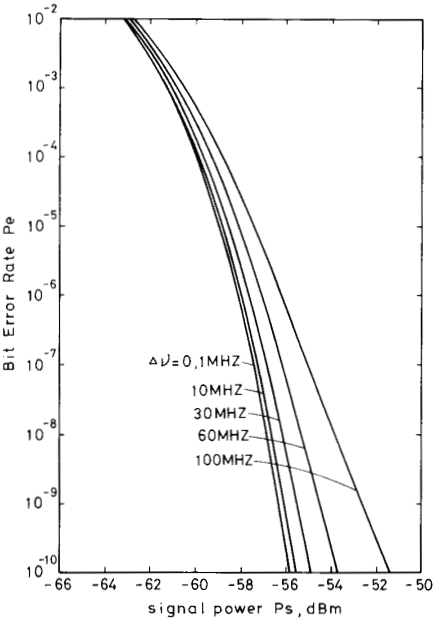

Fig. 5. BER curves for 150-Mbit/s data rate, 550-MHz frequency deviation, and Approximation II of the mixed noise terms.

2) For Case A, BER begins to degrade rapidly when the total linewidth ($\Delta\nu$) exceeds 10 MHz. It is also obvious that a noise floor exists (Figs. 2 and 3) such that a BER of 10^{-7} (or smaller) cannot be achieved for $\Delta\nu$ = 60, 100 MHz.

3) For Case B, with twice the frequency deviation of case A, BER degradation is much improved and a BER of 10^{-9} can be achieved even for $\Delta\nu$ = 100 MHz at a P_s level no greater than -53 dBm. No noise floor appears on the plot.

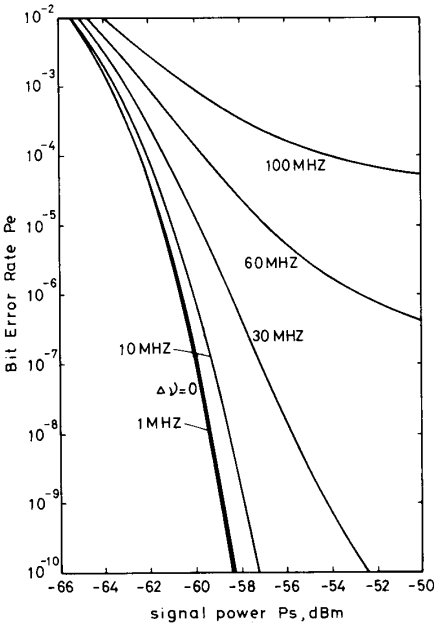

Fig. 6. BER curves of the single branch receiver, all parameters being the same as the case in Fig. 2.

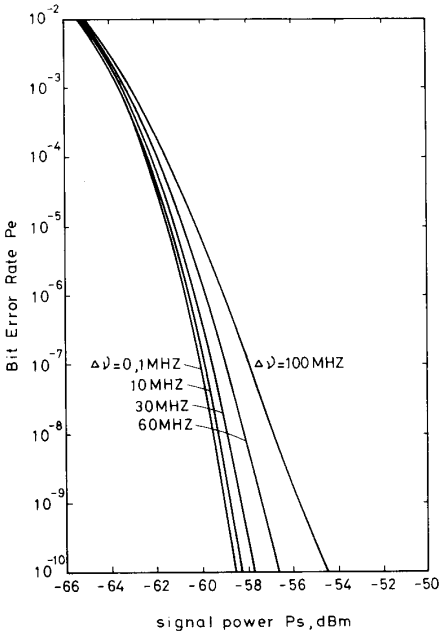

Fig. 8. BER curves of the single branch receiver, all parameters being the same as the case in Fig. 4.

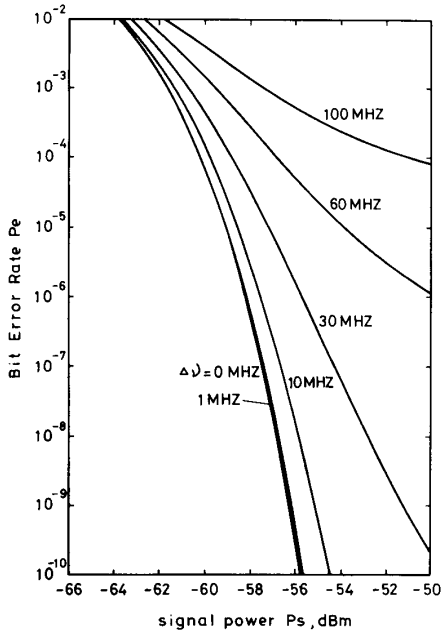

Fig. 7. BER curves of the single branch receiver, all parameters being the same as the case in Fig. 3.

Special Case: The single branch receiver: If polarization matching is achieved by some other means (e.g., by using a polarization maintaining fiber), then our receiver reduces to the single branch structure proposed in [7]. The numerical BER results have also been evaluated for the two frequency deviations (275 MHz, 550 MHz) and two different approximations for the "mixed" noise terms. (Figs. 6 and 7 for f_d = 275 MHz; Figs. 8 and 9 for f_d = 550 MHz).

It can be expected that the single branch receiver has better performance because of the smaller shot noise power. Comparing Figs. 6–9 with Figs. 2–5 indeed confirms this, but the improvements are less than 1 dB and even negligible especially when $\Delta\nu$ is large. Similar conclusions have been obtained for heterodying FSK receivers [9] with nonlimiting IF stages.

V. Conclusion

We have studied a polarization-insensitive optical phase-diversity FSK receiver based on the extension of an experimentally demonstrated design [7]. The advantage is that neither polarization maintaining fibers nor electromechanical polarization control is necessary. We have analyzed the performance of this receiver structure by using two slightly different approximations for the "mixed" noise terms in the frequency discriminator output and by assuming the total noise statistics to be Gaussian. The results indicate that, although more complicated in structure, this polarization-insensitive receiver performs almost equally well compared with the original simpler one (i.e., without polarization diversity) and a BER of 10^{-9} for a 150-Mbit/s data rate can be achieved at a received power level no greater than −53 dBm with a frequency deviation ratio of approximately 4. The per-

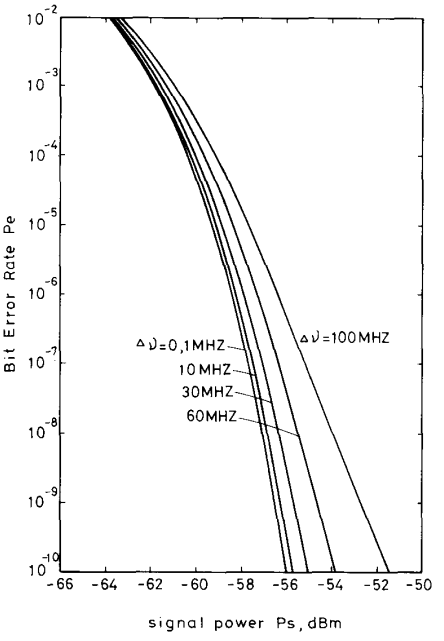

Fig. 9. BER curves of the single branch receiver, all parameters being the same as the case in Fig. 5.

formance is also found to be independent of the power division ratio of the received signal along the two (vertical and horizontal) axes. Finally, such performance can be expected in practical implementations only if 1) the local oscillator power is large enough to suppress the thermal noise and 2) component characteristics (including time delays) in each branch are well matched.

Appendix
Partial Check for the Accuracy of the Gaussian Approximation

Due to the complicated forms of $v_d(t)$ (discriminator output) and $v_0(t)$ [the low-pass filtered version of $v_d(t)$], we have to assume Gaussian distribution and use some additional approximations to obtain expressions for the BER in closed forms. Questions may naturally arise concerning the validity of such approximations. To verify their accuracy, we have done some numerical simulations described in this Appendix.

A. Simulation and Results

We have chosen the Monte Carlo approach for the simulation. Although it is very CPU time consuming, its degree of accuracy does not depend on the actual probability density functions (pdf) (which are unknown in our case) of the random signals being simulated. Due to the limitation in our computing facilities, we are subjected to the following restrictions.

1) Only the single-branch (i.e., no polarization-diversity) receiver is simulated. There may be, however, little loss in generality since the noise terms arising in the vertical and the horizontal branches have the same mathematical forms.

2) The total linewidth $\Delta\nu$ is fixed at 60 MHz, a reasonable value for DFB laser diodes commercially available at present.

3) Only BER greater than 2×10^{-5} has been simulated [15].

The simulation is done on 6 MIPS 80386 PC workstations using the MATLAB™ software. This package has been adopted because of its array (vector) processing capability and extensive built-in signal processing (filtering, random noise generation, etc.) functions.

The simulation procedure is similar to the one described in [15]. All function blocks of the receiver were simulated and care has been taken to ensure the mutual independence of all noise sources. The low-pass filters LPF_A and LPF_B are all taken to be second-order Butterworth type with bandwidths indicated in the text.

Figs. 10 and 11 show the simulated and theoretically predicted BER's for the single-branch receiver with data rate 150 Mbits/s, total linewidth 60 MHz, and frequency deviations 275 MHz and 550 MHz, respectively. 90-percent confidence intervals are also indicated for all the simulated BER's.

Fig. 12(a) shows the simulated and predicted Gaussian (Approximation II) distribution of the sample values of the detector output $v_0(kT)$ for a frequency deviation of 275 MHz and received signal level of -62 dBm (BER $\approx 10^{-2}$). The portion of the curves near decision threshold (zero) is shown in magnified form in Fig. 12(b).

B. Discussion

From the simulated data we can see that the approximations made in deriving the theoretical results are realistic, at least for BER's in the range from 10^{-2} to 10^{-5}. There is one thing that remains to be explained: for a BER greater than $\approx 10^{-2}$ the simulated error rate may be higher than the "upper bound" (Approximation II). This can be understood by seeing that, although an upper bound has indeed been found for $v_0(t)$, the distribution of this upper bound is not exactly Gaussian, as was assumed. Such deviations are not important, however, since no practical systems operate at so high an error rate.

To simulate system performance at bit error rates lower than 10^{-5}, one has to either use very fast vector computers or employ the importance sampling technique, which reduces the required sample size. The former may extend the obtainable BER to $\approx 10^{-7}$ with reasonable CPU time. The latter has been used to simulate BER's lower than 10^{-9}, but the results can be fully justified only if the pdf's are known approximately.

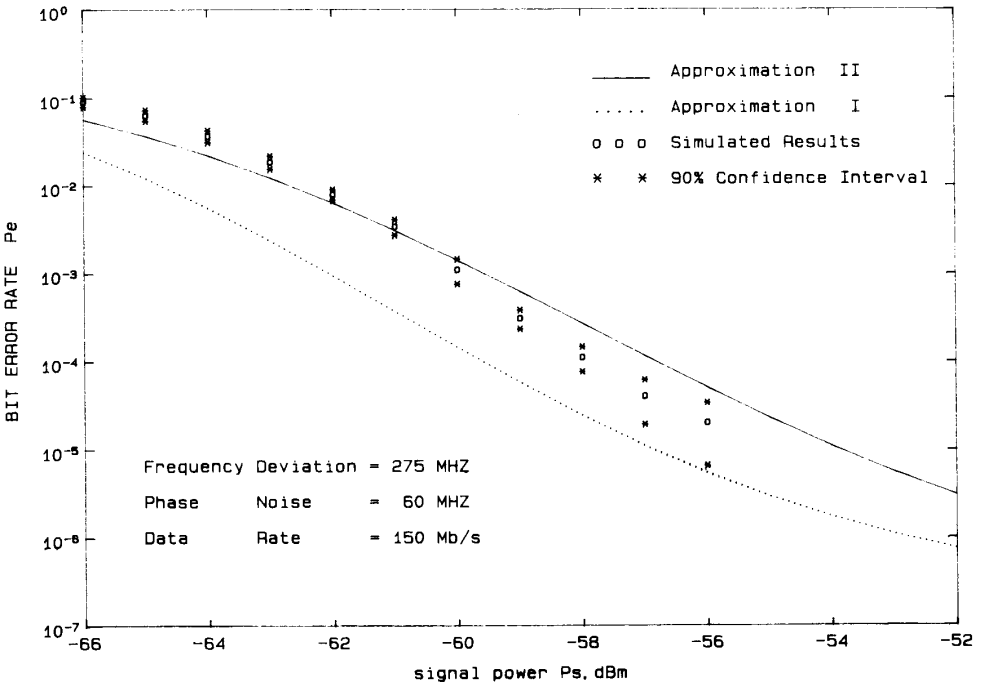

Fig. 10. Simulated and theoretically predicted (Approximations I and II) BER for the single-branch (phase-diversity only) receiver, data rate = 150 Mbits/s, total linewidth $\Delta\nu$ = 60 MHz, f_d = 275 MHz.

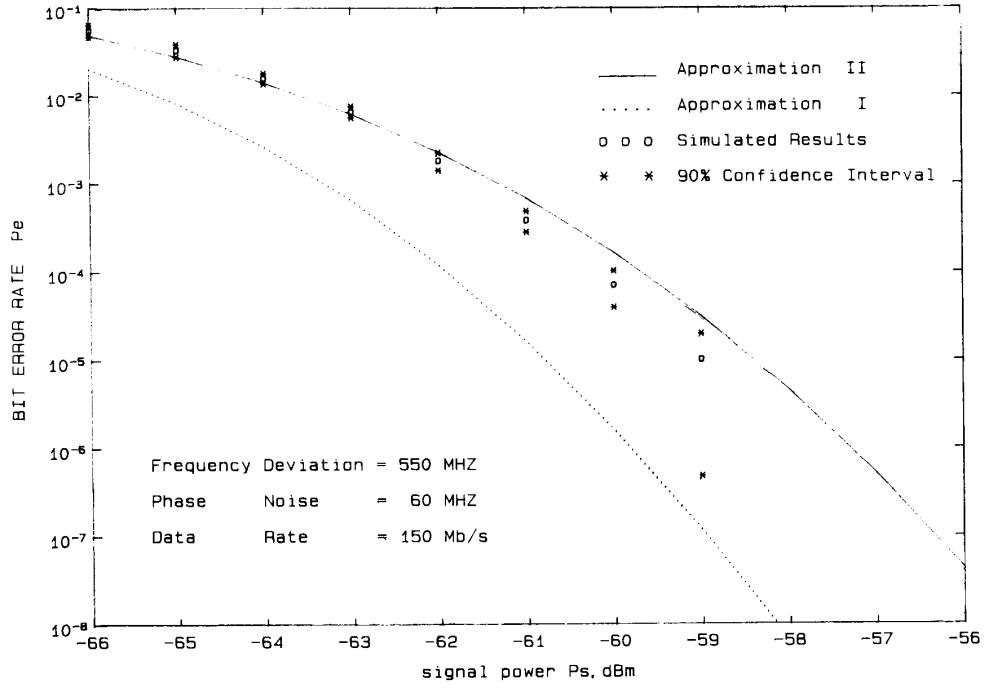

Fig. 11. Same as Fig. 10, but with f_d = 550 MHz.

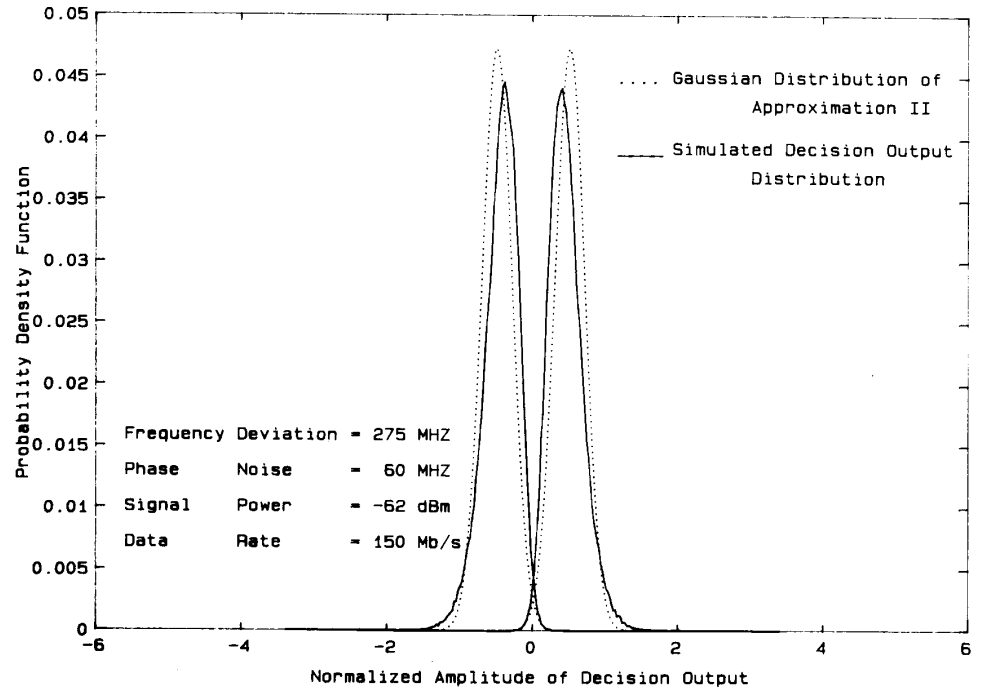

(a)

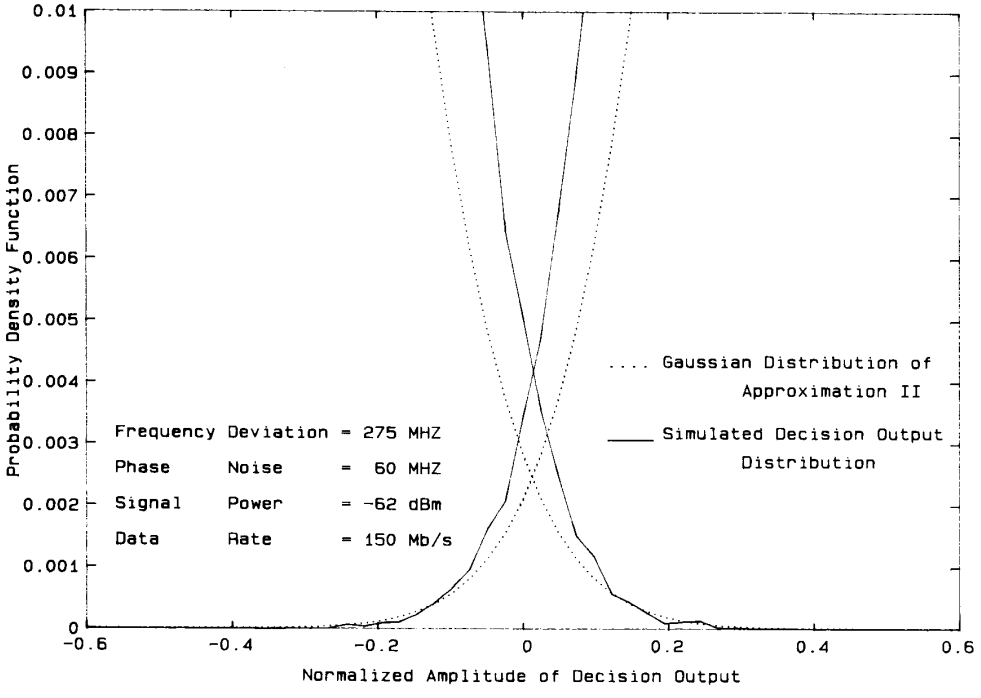

(b)

Fig. 12. (a) Simulated and predicted Gaussian (Approximation II) pdf for the single-branch (phase-diversity only) receiver, data rate = 150 Mbits/s, $\Delta\nu$ = 60 MHz, f_d = 275 MHz, P_s = − 62 dBm. (b) Same as (a), but only the magnified central portion is shown.

REFERENCES

[1] T. Kimura, "Coherent optical fiber transmission," *J. Lightwave Technol.*, vol. LT-5, no. 4, pp. 414–428, 1987.

[2] I. Garrett and G. Jacobsen, "The effect of laser linewidth on coherent optical receivers with nonsynchronous demodulation," *J. Lightwave Technol.*, vol. LT-5, no. 4, pp. 551–560, 1987.

[3] I. Garrett and G. Jacobsen, "Influence of laser linewidth on the error-rate floor in dual filter optical FSK receivers," *Electron. Lett.*, vol. 21, pp. 268–270, 1985.

[4] G. Nicholson, "Transmission performance of an optical FSK heterodyne system with a single-filter envelope-detection receiver," *J. Lightwave Technol.*, vol. LT-5, no. 4, pp. 502–508, 1987.

[5] R. S. Vodhanel, B. Enning, and A. F. Elrefaie, "Bipolar optical FSK transmission experiments at 150 Mbit/s and 1 Gbit/s," *J. Lightwave Technol.*, vol. 6, no. 10, pp. 1549–1553, 1988.

[6] A. W. Davis, M. J. Pettitt, J. P. King, and S. Wright, "Phase diversity technique for coherent optical receivers," *J. Lightwave Technol.*, vol. LT-5, no. 4, pp. 561–572, 1987.

[7] R. Noé, W. B. Sessa, R. Welter, and L. G. Kazovsky, "New FSK phase-diversity receiver in a 150 Mbit/s coherent optical transmission system," *Electron. Lett.*, vol. 24, no. 9, pp. 567–568, 1988.

[8] B. Glance, "Polarization independent coherent optical receiver," *J. Lightwave Technol.*, vol. LT-5, no. 2, pp. 274–276, 1987.

[9] M. Kavehrad and B. Glance, "Polarization-insensitive FSK optical heterodyne receiver using discriminator demodulation," *J. Lightwave Technol.*, vol. 6, no. 9, pp. 1386–1394, 1988.

[10] H. W. Tsao, J. Wu, and Y. H. Lee, "Performance analysis of optical phase diversity FSK receiver using delay-and-multiplying discriminators," *J. Optical Commun.*, to be published.

[11] T. Okoshi and K. Kikuchi, *Coherent Optical Fiber Communications*. Norwell, MA: Kluwer Academic Publishers, 1988, ch. 3.

[12] P. Z. Peebles, Jr., *Digital Communication Systems*. Englewood Cliffs, NJ: Prentice-Hall, 1987, ch. 4.

[13] R. E. Ziemer and W. H. Tranter, *Principles of Communication*, 2nd ed. Boston, MA: Houghton-Mifflin, 1985, ch. 7.

[14] R. E. Ziemer and R. L. Peterson, *Digital Communication and Spread Spectrum Systems*. New York: Macmillian, 1985, ch. 3.

[15] L. G. Kazovsky, P. Meissner, and E. Patzak, "ASK multiport optical homodyne receivers," *J. Lightwave Technol.*, vol. LT-5, no. 6, pp. 770–791, 1987.

*

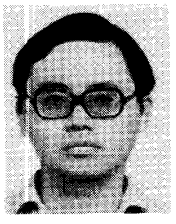

Hen-wai Tsao (M'78–S'89) received the B.S. and M.S. degrees in electrical engineering from National Taiwan University, Taipei, Taiwan, Republic of China, in 1975 and 1978, respectively.

He joined the faculty of the Department of Electrical Engineering, National Taiwan University in 1978 and became an Associate Professor in 1983. His main research interests are optical fiber communication system and communication electronics. He is currently a candidate for the Ph.D. degree in electrical engineering.

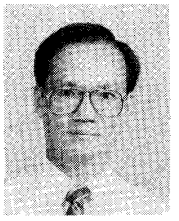

Jingshown Wu (S'73–M'78) received the B.S. and M.S. degrees in electrical engineering from National Taiwan University, Taipei, Taiwan, Republic of China, and the Ph.D. degree from Cornell University, Ithaca, NY, in 1970, 1972, and 1978, respectively.

He jointed Bell Laboratories in 1978, where he worked on digital network standards and performance, and optical fiber communication systems. In 1984 he jointed National Taiwan University as a Professor. He is interested in optical fiber communication systems, optical fiber signal processing, and computer communication networks.

Dr. Wu is a member of the Chinese Institute of Engineers/USA, Phi Kappa Phi, the Optical Society of China, and the Institute of Chinese Electrical Engineers.

*

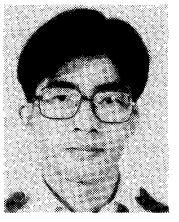

Shien-Chi Yang was born in Taiwan, Republic of China, in 1963. He received the B.S. degree in electrical engineering from National Taiwan University, Taipei, Taiwan, in 1986. Currently, he is pursuing the M.S. degree at the Institute of Electrical Engineering, National Taiwan University.

From 1986 to 1988, he joined the Air Force, working on the maintenance of digital switching systems. His main research interests are in the areas of optical fiber communication systems, especially in the computer simulation of coherent optical communication systems.

*

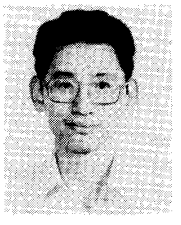

Yang-Han Lee was born in Taipei, Taiwan, Republic of China, on February 11, 1964. He received the B.S. and M.S. degrees in electrical engineering from National Taiwan University, Taipei, Taiwan, in 1987 and 1989, respectively.

He is currently studying toward the Ph.D. degree in electrical engineering at the National Taiwan University. His research interests are in the area of optical fiber communication systems.